

## DEVELOPING TURBULENT FLOW IN A SIMULATED ROD BUNDLE

Aidir Parizzi Jr. and Sergio V. Möller

Programa de Pós-Graduação em Engenharia Mecânica - PROMEC  
 Universidade Federal do Rio Grande do Sul - UFRGS  
 Rua Sarmento Leite, 425  
 90050-170 - Porto Alegre, RS, Brazil  
 e-mail: svmoeller@vortex.ufrgs.br

### SUMMARY

*In this paper, the turbulent flow in the entrance region of a simulated rod bundle is investigated. The test section consists of a 4-rod bundle, in square arrangement, with a pitch-to diameter ratio  $P/D = 1.15$ . Measurements of velocity were made by means of Pitot tubes and hot wires. Dimensionless results show that the development of the velocity profiles is influenced, as expected, by the walls, due to the non-slip condition. It is strongly influenced by the narrow gaps as well, so that in that region, the particular features of the flow development in rod bundles starts.*

### INTRODUCTION

Rod bundles are the most common geometry of nuclear reactors fuel elements. The heat generated by the nuclear reaction is removed by the coolant, usually in turbulent flow parallel to the rods. The design of the fuel elements requires the solution of the conservation equations for mass, momentum and energy, to arrive at their safe and reliable operation. Detailed experimental data of velocity, turbulence and temperature are, therefore, necessary for turbulence modeling and code validation.

With this purpose, a lot of effort has been devoted in the last years to obtain experimental results from the turbulent flow in rod bundles, showing that the structure of the fully developed turbulent flow in this type of channel differs strongly from the flow in pipes (Rehme, 1987-a). This is due to a process of quasi-periodic flow pulsations in the narrow gaps between the rods, which is responsible for the mass and heat exchange between adjacent subchannels (mixing) and, due to its features, can induce vibrations on the rods (Möller, 1988, 1991, 1992; Wu, Trupp, 1994). The particular geometry of rod bundles is responsible for this phenomenon.

Entrance effects were not considered in most of the experimental studies in the literature, although heat is generated at short distances from rod tip. Heat transfer coefficients in this region are expected to be higher than in other regions and there exist a lack of information for the subsequent structural analysis. The work of Presser, (1967), dealing with heat transfer and pressure drop in rod bundles, is singular in the literature considering entrance effects. It is also the only one in this subject cited by Rehme (1987-b), in his extensive review about flow through rod bundles. Flow visualizations with smoke and a high speed camera, performed by Guellouz and Tavoularis (1995) to complement their hot wire measurements of developed flow in a rectangular channel, where a single rod was placed to simulate the gap region between rod and channel wall, show the presence of flow pulsations even in regions near the entrance.

In this paper, the velocity and velocity fluctuations distributions of the turbulent flow in the entrance region of a simulated rod bundle are

investigated with the purpose of determining the characteristics of the flow development in rod bundles, as presented in more detail in Parizzi (1998).

### APPARATUS AND EXPERIMENTAL TECHNIQUE

The test section, shown in Figure 1, consists of a 4-rod bundle, in square arrangement, with a pitch-to diameter ratio  $P/D = 1.15$ , placed in a 1370 mm long rectangular sleeve, with 146 mm height and a width of 193 mm. This sleeve could be slidden in the main channel, with rectangular cross section, with 146 mm height and a width of 193 mm to create the entrance conditions by inserting the rod bundle at different lengths.

Air is the working fluid, driven by a centrifugal blower, passed by a settling chamber and a set of honeycombs and screens, before reaching the rod bundle with about 2 % turbulence intensity. The rods were hollow with chamfered edges to reduce disturbances effects that might affect the formation of the boundary layer at the entrance and a diameter of 60 mm. One of the rods could be changed, having lengths of 65 mm ( $L/D_h = 1.62$ ), 350 mm ( $L/D_h = 8.65$ ), 550 mm ( $L/D_h = 13.59$ ) and 800 mm ( $L/D_h = 19.77$ ). At the external extremity of the rod measurement probes were placed, allowing measurements of air flow velocity and turbulence intensities at about 30 mm before the outlet of the rectangular channel. Measurements were performed in a quadrant of the subchannel, as shown, schematically in Fig. 2 for the Pitot tube.



Figure 1: General view of the test section. Flow is from right to left.

Wall shear stresses were measured by a Preston tube (Patel, 1965), while a Pitot tube was used for velocity measurements. Both had 1.3 mm external diameter and were connected to a Hartmann & Braun ARA 500 pressure transmitter. Velocity and velocity fluctuations in axial direction were measured by means of a DANTEC *StreamLine* hot wire anemometer. Axial velocity and its fluctuations were measured with a "boundary-layer" hot wire probe, with a single wire perpendicular to the direction of the main flow. The results of the measurements were directly evaluated with the help of the software *StreamWare*.

The Pitot tube or the hot wire probe were mounted in the extremity of the rod with variable length, as shown in Fig. 3. This positioning device allowed the radial displacement of the probes, with help of a micrometer, perpendicular to the rod wall. It could also be rotated, so that the measurements of velocity and velocity fluctuations could be performed at various angles, covering 90° starting from the lower narrow gap between the rods. This procedure allowed measurement of these quantities in one quadrant representative of the central subchannel of the test section.

Data acquisition was carried out with help of a Keithley DAS-58 A/D converter board connected to a personal computer, with a sampling frequency of 50 kHz and a time record of 10 seconds.

## RESULTS

### Velocity Field

Figure 3-a-d shows the dimensionless velocity profile. The measured velocities are scaled by the mean friction velocity, given by the local wall shear stress  $\tau_w$  and the fluid density  $\rho$ , as

$$u^* = \sqrt{\tau_w / \rho} \quad (1)$$

Hence, the dimensionless velocity  $u^*$  will be defined as

$$u^+ = \bar{U} / u^* \quad (2)$$

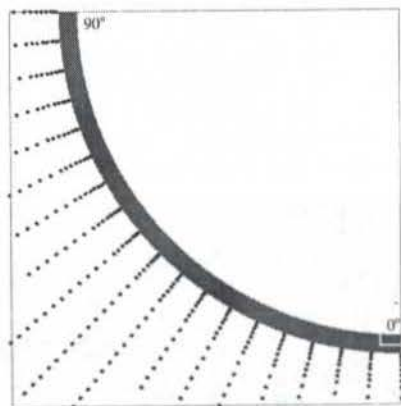


Fig. 2 Schematic view of the subchannel quadrant with the points for velocity measurement with the Pitot tube.

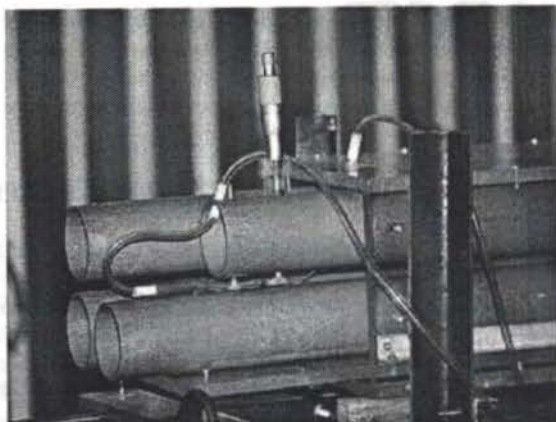


Figure 2: Detail of the outlet of the test section, showing the instrumented tube and the micrometric positioner with the Pitot tube placed at the lower gap (0°).

and presented as a function of the dimensionless distance from the wall

$$y^+ = \frac{yu^*}{\nu} \quad (3)$$

where  $y$  is the distance from the wall and  $\nu$  the kinematic viscosity.

Overbars will denote, henceforth, time averaged quantities.

For comparison, as a continuous line Nikuradse's "Law of the Wall" (Nikuradse, 1936) distribution of the time-averaged velocity of the turbulent isothermal flow in a smooth pipe, is also shown, given by

$$u^+ = 2.5 \ln y^+ + 5.5 \quad (4)$$

As the  $L/Dh$  ratio increases, experimental points approach Nikuradse's curve. The influence of the free stream in the channel is gradually reduced as the constant dimensionless velocity values at higher  $y^+$  values start to follow the slope of the Law of the Wall. The flow is not completely developed at the largest  $L/Dh$  ratio, although in the regions of the narrow gaps between the rods the boundary layer formation is complete, since all data points of the angles 0° to 20° and 75° to 90° follow the Law of the Wall.

The same velocity fields, scaled with the reference velocity are presented as contours in figures 4-a-d. The smallest  $L/Dh$  ratio shows very high velocity gradients near the walls and the region of constant velocity in the center of the subchannel observed in Fig. 3. As the  $L/Dh$  ratio increases, velocity gradients near the walls are reduced, while the velocity near the center of the subchannel increases and, from the narrow gaps toward the center of the subchannel, velocity gradients parallel to the walls are being formed. The latter is the condition of existence of flow pulsations between the subchannels (Möller, 1988, 1992), which may indicate that mixing takes place at short distances from the entrance.

### Turbulence Measurements

The normal components of the Reynolds stress tensor are usually presented in form of turbulence intensities, i.e. the square root of the mean square value of the component of the velocity fluctuation in axial, radial and azimuthal directions, respectively, scaled with the friction velocity. Figure 5-a-d shows the distribution of the axial component, given by

$$\sqrt{u'^2}/u^*$$

For comparison, results for pipe flow are presented as a dotted line (Lawn, 1971).

In the entrance, experimental values of axial turbulence intensities are scattered, showing the influence of the channel turbulence. As the  $L/Dh$  ratio increases, experimental points tend to approach pipe flow results, although some scattering is still observed for the largest  $L/Dh$  ratio, indicating again that the flow is not entirely developed. On the other side, in the regions of the narrow gaps the data points follow the same distribution of the fully developed pipe flow. Near the largest distance from the wall, at  $20-25^\circ$  and  $75^\circ$  a small growth of the turbulence intensities is observed, similar to the results of Rehme (1986) indicating the presence of flow pulsations (Möller, 1988, 1991).

### Spectral analysis

The Fourier Analysis is a valuable tool for the study of random phenomena being widely applied to turbulence studies. Usually, random data are presented in form of time series, representing a continuous (analog) function of time, sampled for digital analysis with a frequency  $f$  as a sequence of numbers at regular time intervals.

The autospectral density function (or power spectrum) represents the rate of change of the mean square value of a certain time function  $x(t)$  with the frequency  $f$  (Bendat and Piersol, 1986).

$$\phi_{xx}(f) = \frac{1}{B\theta} \int_0^\theta x^2(f, B, t) dt \quad (5)$$

where  $\theta$  is an adequate integration (observation) time and  $B$  the bandwidth.

In the Fourier space, the autospectral density function will be defined as the Fourier transform of the autocorrelation function  $R_{xx}(t)$ , defined as the mean value of the product of this function at a time  $t$ , with its value at a time  $t+\tau$ .

Let  $x(t)$  be a generic function of time, so that a correlation function of  $x(t)$  can be written as

$$R_{xx}(\tau) = \frac{1}{\theta} \int_0^\theta x(t)x(t+\tau) dt \quad (6)$$

The function defined via equation (6) is called autocorrelation function, when divided by the mean square value of  $x(t)$ , will be called autocorrelation coefficient function, noted by  $C_{xx}$ . The autospectral density will be given by

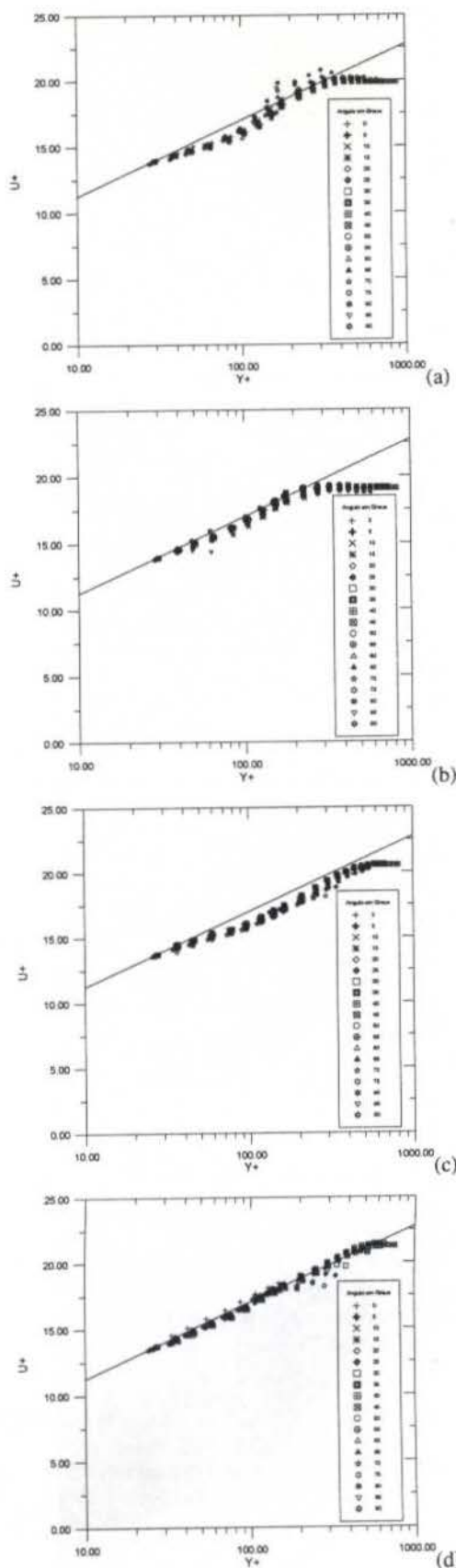


Fig. 3: Dimensionless logarithmic velocity field: (a)  $L/Dh = 1.2$ , (b)  $L/Dh = 5.8$ , (c)  $L/Dh = 9.5$ , (d)  $L/Dh = 13.5$ .

Fig. 4: Velocity field as contours: (a)  $L/Dh = 1.2$ , (b)  $L/Dh = 5.8$ , (c)  $L/Dh = 9.5$ , (d)  $L/Dh = 13.5$ .

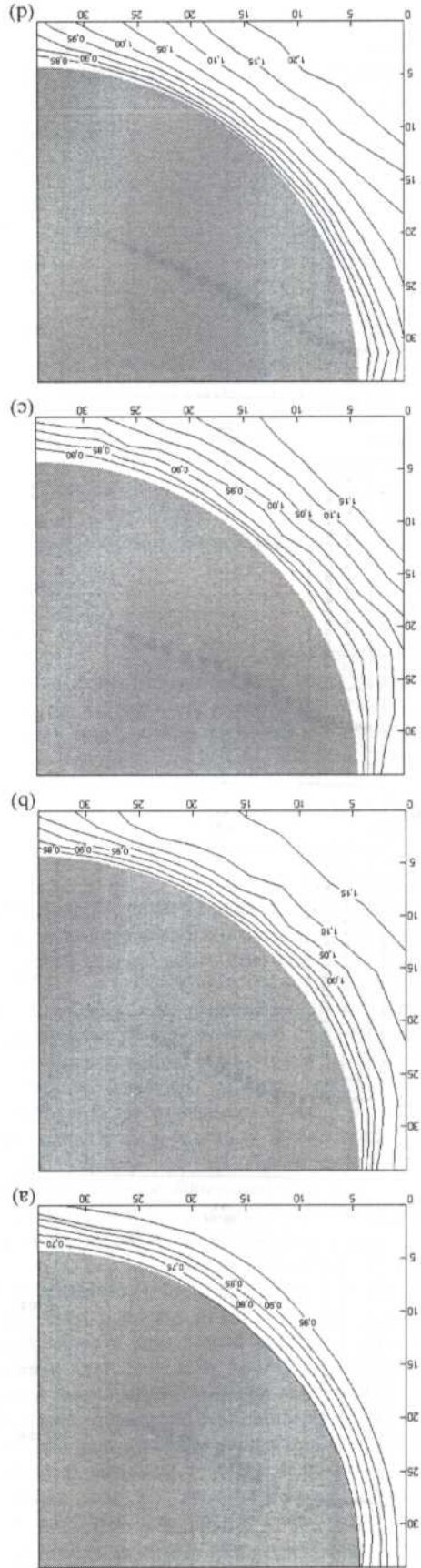
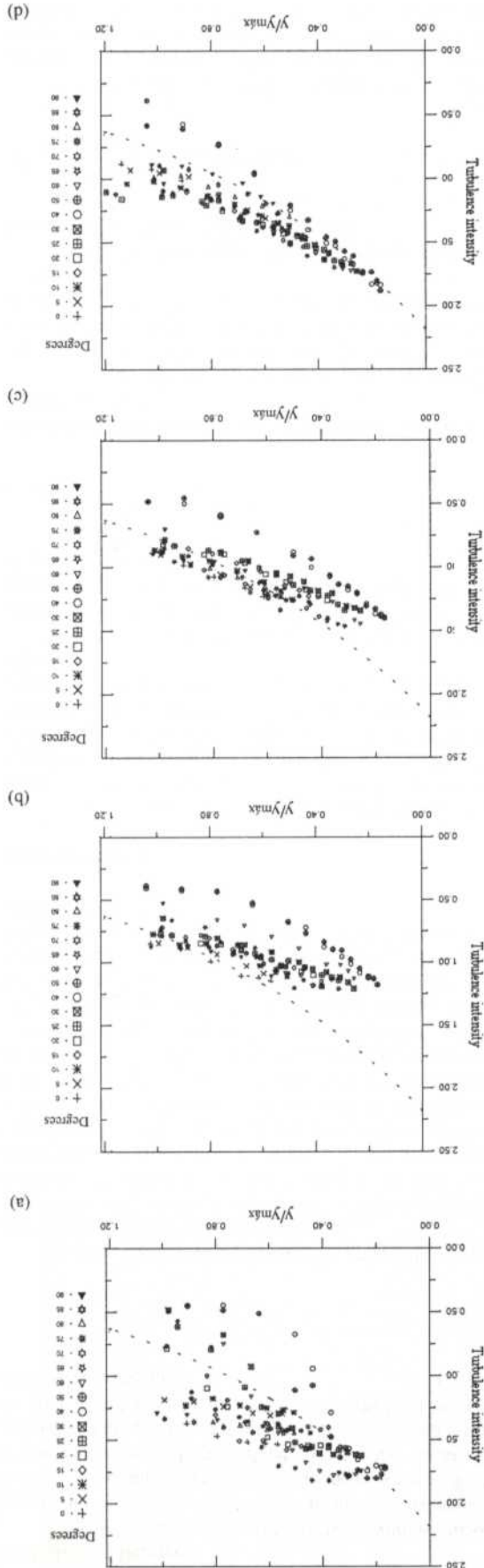


Fig. 5: Axial turbulence intensities: (a)  $L/Dh = 1.2$ , (b)  $L/Dh = 5.8$ , (c)  $L/Dh = 9.5$ , (d)  $L/Dh = 13.5$ .



$$\phi_{xx}(f) = \int_{-\infty}^{+\infty} R_{xx}(t) e^{-i2\pi f t} dt \quad (7)$$

In this research work, time function  $x(t)$  is the axial velocity fluctuation of the flow.

The autospectral density for the position at  $\theta = 65^\circ$ ,  $L/Dh = 13.5$ , is shown in Fig. 6. The choice of this measuring point is based on results by Rehme (1987-a), Möller (1988, 1991) and Wu and Trupp (1994) that show that flow pulsations appear in the axial direction at locations where a small growth of this component of the turbulence intensity is observed near the largest distance from the wall. The analysis of the spectra in all  $L/Dh$  ratios allows to identify the small peak at about  $40^\circ$  as produced by the rod bundle, other peaks are attributed to the channel, since they appear in all spectra measured, with decreasing intensity as the  $L/Dh$  ratios increase.

This frequency can also be identified in the plot of the autocorrelation, Fig. 7, where this function presents an oscillation with a period of about 20 to 25 ms, corresponding to a frequency of 40 to 50 Hz. By calculating a Strouhal number with the hydraulic diameter and the friction velocity at the nearest gap, a value of  $Str = 4.72$  is obtained, 17% lower than the value obtained for this  $P/D$  ratio ( $Str = 5.69$ ) through the relation (Möller, 1988, 1991)

$$Str^{-1} = 0.808 \frac{S}{D} + 0.056 \quad (8)$$

where  $S$  is the gap width ( $P-D$ ).

## CONCLUSIONS

This paper presents the experimental study of the flow development in one quadrant of a subchannel of a simulated rod bundle.

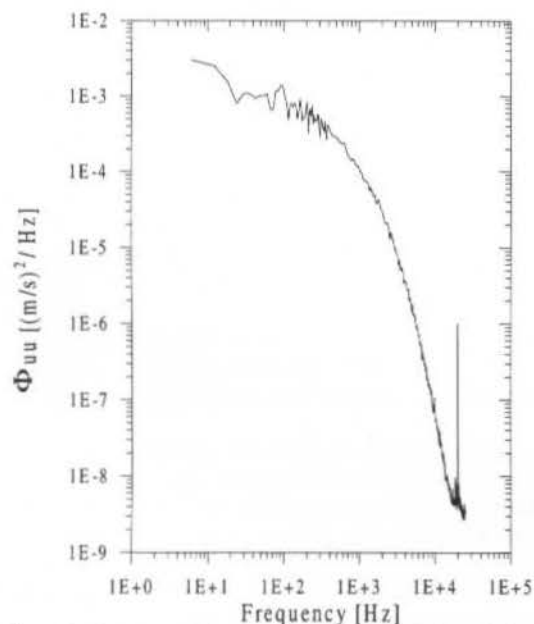


Fig. 6: Autospectral density of the axial turbulence intensity at  $\theta = 65^\circ$ ,  $L/Dh = 13.5$ .

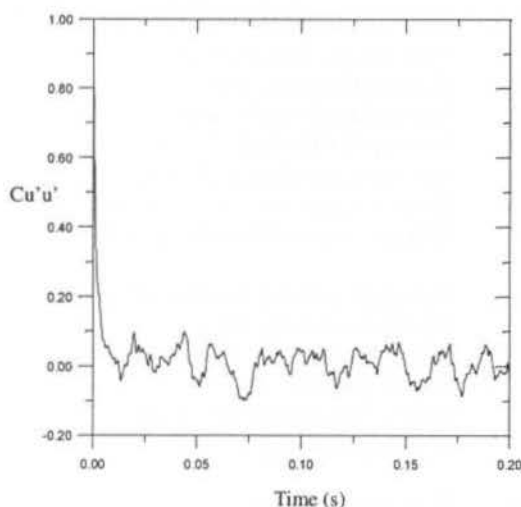


Fig. 7: Autocorrelation function of the axial turbulence intensity at  $\theta = 65^\circ$ ,  $L/Dh = 13.5$ .

Dimensionless results show that the development of the velocity profiles is influenced, as expected, by the walls, due to the non-slip condition. It is strongly influenced by the narrow gaps as well, so that in that region, the particular features of the flow development in rod bundles starts.

Results of axial turbulence intensities and of autospectral densities and autocorrelation functions show that the phenomenon of flow pulsations, responsible for the mass exchange between subchannels starts during the flow development.

This study considered only entrance effects due to the boundary layer formation on the rods, since they were hollow to avoid entrance effects due to flow acceleration around plugs in their extremities or other structural elements like perforated plates, as in actual fuel elements. Future work will consider this aspect. Effects of flow redistribution due to asymmetric entrance conditions will also be studied.

## ACKNOWLEDGEMENTS

The support of CNPq - Brazilian Scientific and Technological Council, through the grant 400180/92-8, is gratefully acknowledged.

Aidir Parizzi Jr. thanks also the CAPES / Ministry of Education, Brazil, for granting him a fellowship.

## LIST OF SYMBOLS

$C_{u'u'}$	Autocorrelation function - $(m/s)^2$ .
$D$	Rod diameter - m.
$f$	Frequency - Hz.
$P$	Pitch - m.
$R_{u'u'}$	Autocorrelation coefficient function.
$Re$	Reynolds number $(U_m D_e / \nu)$ .
$S$	Gap width ( $P-D$ ) - m.
$Str$	Strouhal number $(f.D/u^*)$ .
$t$	Time - s.

$\bar{U}$	Axial velocity - m/s.
$u'$	Axial velocity fluctuation - m/s.
$U_m$	Mean axial velocity - m/s.
$U_{max}$	Maximal axial velocity - m/s.
$u^*$	Friction velocity $(\tau_w/\rho)^{-1/2}$ - m/s.
$u^+$	Dimensionless velocity $(\bar{U}/u^*)$ .
$y$	Distance to pipe wall - m.
$y^+$	Dimensionless wall distance $(yu^*/\nu)$ .
$\Phi_{u'u'}$	Autospectral density function - $(m/s)^2/Hz$ .
$\nu$	Kinematic viscosity - $m^2/s$ .
$\rho$	Density - $kg/m^3$ .
$\theta$	Angular position - deg.
$\tau$	Time lag for autocorrelations - s.
$\tau_w$	Wall shear stress - Pa.
$\sqrt{u'^2}/u^*$	Turbulence intensity.

Rehme, K., 1987-b, "Convective heat transfer over rod bundles", Handbook of Convective Heat and Mass Transfer, S. Kakaç, R. K. Shah, W. Aung Eds., Chap. 7, pp. 7\_1-7\_62.

Wu, X. and Trupp, A. C., 1994, "Spectral measurements and mixing correlation in simulated rod bundle subchannels", Int. J. Heat Mass Transfer, Vol. 37, pp. 1277-1281.

**Keywords:** Turbulent flow, rod bundles, hot wires.

## REFERENCES

Bendat, J. S. and Piersol, A. G., 1986, "Random Data: analysis and measurement procedures", Wiley, New York.

Guellouz, M. S. and Tavoularis, S., 1995, "Large-scale transport across narrow gaps in rod bundles", Proc. NURETH 7 - 7th Int. Conf. on Reactor Thermal Hydraulics, Saratoga Springs.

Hinze, O., 1975, "Turbulence", McGraw-Hill, New York.

Lawn, C. J., 1971, "The determination of the rate of dissipation in turbulent pipe flow", J. Fluid Mechanics, Vol. 48, pp. 477-505.

Möller, S. V., 1988, "Experimentelle Untersuchung der Vorgänge in engen Spalten zwischen den Unterkanälen von Stabbündeln bei turbulenter Strömung", Dr.-Ing. Dissertation, Universität Karlsruhe (TH), Karlsruhe (also: KfK 4501, 1989).

Möller, S. V., 1991, "On phenomena of turbulent flow through rod bundles", Exp. Thermal Fluid Science, Vol. 4, pp. 25-35.

Möller, S. V., 1992, "Single-phase turbulent mixing in rod bundles", Exp. Thermal Fluid Science, Vol. 5, pp. 26-33.

Nikuradse, J., 1932, "Gesetzmässigkeit der turbulenten Strömung in glatten Röhren", VDI-Forschungsheft 356.

Parizzi Jr., A., 1998, "Desenvolvimento do escoamento axial turbulento nos subcanais de feixes de barras", Dissertação de Mestrado, PROMEC/UFRGS, Porto Alegre-RS.

Patel, V. C., 1965, "Calibration of the Preston tube and limitations on its use in pressure gradients", J. Fluid Mech., Vol. 23, pp. 185-208.

Presser, K., 1967, "Wärmeübergang und Druckverlust an Reaktorbrunnenelementen in Form längsdurchströmter Rundstabbündeln", Jül-486-RB, Kernforschungsanlage Jülich, Jülich.

Rehme, K., 1986, "Turbulenzstruktur im Wandkanal eines Stabbündels ( $P/D=W/D=1.148$ ) für drei Ebenen im Einlauf", KfK 4027, Kernforschungszentrum Karlsruhe, Karlsruhe.

Rehme, K., 1987-a, "The structure of turbulent flow through rod bundles", Nuclear Eng. Des., Vol. 99, pp. 141-154.